Micro- and Meso-Scale Analyses for Quantifying Hypoxemia in Methemoglobinemia

Tanmoy Sanyal and Saikat Chakraborty

***Abstract*— Methemoglobinemia is a disease that results from abnormally high levels of methemoglobin (MetHb) in the red blood cell (RBC) caused by simultaneous uptake of oxygen (O_2) and nitric oxide (NO) in the human lungs. MetHb is produced in the RBC by irreversible NO-induced oxidation of the oxygen carrying ferrous ion (Fe^{2+}) in the heme group of the hemoglobin (Hb) molecule to its non-oxygen binding ferric state (Fe^{3+}). In this paper, we study the role of NO in the pathophysiology of methemoglobinemia by performing a multiscale quantitative analysis of the relation between levels of NO inhaled by the patient and the hypoxemia resulting from the disease. Reactions of NO occurring in the RBC with both Hb and oxyhemoglobin are considered in conjunction with the usual reaction between oxygen and Hb to form oxyhemoglobin. Our dynamic simulations of NO and O_2 uptake in the RBC and in the plasma in pulmonary capillaries under continuous, simultaneous exposure to both gases reveal that at the end of the pulmonary transit time of 1 s, the oxygen saturation in the RBC equilibrates at 97% in absence of NO but it shows a steady decline to 95% as the concentration of NO increases to 50 ppm. We further show that NO levels of 150 ppm or higher while breathing in room air may be considered to be fatal for methemoglobinemia patients since it causes severe hypoxemia by decreasing the oxygen saturation to below its critical value of 90%. Our analysis shows that the diagnosis of hypoxemia in methemoglobinemia cannot be done by measuring oxygen partial pressures in the patient's pulmonary artery, but by estimating the oxygen saturation in the patient's erythrocyte using a standard procedure such as pulse oximetry.**

***Index Terms*—nitric oxide, red blood cells, capillary, methemoglobin anemia, hypoxemia**

I. Introduction

Methemoglobinemia is a disorder characterized by the presence of above-normal levels of methemoglobin (MetHb) in the blood. Methemoglobin is a compound formed from hemoglobin (Hb) by oxidation of iron atom from ferrous to ferric state. MetHb lacks the electron needed to form a bond with oxygen, and hence, is incapable of oxygen transport. Generally, red blood cells (RBCs) are continuously exposed to various oxidant stresses and so MetHb is continually produced in humans. Typically, less than 1 percent of the total circulating hemoglobin in a healthy adult is present in the form of MetHb. However, injury or toxic agents convert a larger proportion of hemoglobin into MetHb. In healthy children, the ferric iron in MetHb is readily reduced to the ferrous state through the action of the cytochrome b5 oxidase enzyme (also referred to as methemoglobin reductase), which is present in erythrocytes and other cells.

In this paper, we focus on micro- and meso-scale modeling of Methemoglobinemia. Our analysis comprises of a rigorous formulation and quantification of the variation of the partial pressure and saturation (in RBC) profiles of O_2 and NO caused by convective-diffusive transport in the capillary plasma coupled with diffusive-reactive uptake in the RBC. Continuous exposure of the patient to NO allows the reactions to attain equilibrium, as a result of which the transport of NO through the lung becomes transport-limited. We perform spatial averaging over the volume of the RBC at the micro-scale and over the cross section of the alveolar capillary at the meso-scale using the Liapunov-Schmidt technique of the classical bifurcation theory. The spatially averaged low-dimensional model we obtain is used to quantify the increased Methemoglobin levels inside the RBC, which causes Methemoglobinemia. We also estimate the levels of inhaled NO that could be fatal.

The reactions that occur inside the human RBC in presence of NO and O_2 are given by

$$Hb + O_2 \Leftrightarrow Hb(O_2)_n \quad (1)$$

$$HbO_2 + NO \Leftrightarrow MetHb + NO_3^- \quad (2)$$

$$Hb + NO \Leftrightarrow HbNO \quad (3)$$

In eqn. 1, the Oxygen-Hb equilibrium is assumed to follow the Hill equation, where n is the Hill coefficient (=2.37) and the equilibrium rate constant (K_1) is given by

$$K_1 = \left(H / P_{50}\right)^n, \quad (4)$$

where H= 7.4 x 10^5 Torr and P_{50}= 26 Torr. The reaction rate constant for NO induced oxidation of oxyhemoglobin to MetHb (given by eqn. 2) was calculated by Eich and co-workers [1]. Sheele et al. [2] reported the reaction rate constant for the reaction between NO and deoxyhemoglobin (eqn. 3) as $2x10^7$ $M^{-1}s^{-1}$, and also measured the dissociation rate of Nitrosylhemoglobin. The dissociation rate constant of MetHb (in eqn. 2) is obtained to be 2.47 $x10^{-3}$ s^{-1} [3, 4].

In normal RBCs, MetHb is maintained at a level of less than 1% of total hemoglobin through two metHb-reducing pathways [5, 6]. One of these systems is the redox cycle consisting of cytochrome b5 (cytb5) and cytochrome b5-metHb reductase (b5R), which uses NADH for electron transfer to cytb5 ("cytb5-NADH system"). The other

Manuscript was received on February 8, 2011. This work was performed at the Department of Chemical Engineering, Indian Institute of Technology – Kharagpur, Kharagpur 721302, INDIA.

Tanmoy Sanyal is an undergraduate student of Chemical Engineering at the Indian Institute of Technology – Kharagpur, Kharagpur 721302, INDIA.

Saikat Chakraborty is Assistant Professor of Chemical Engineering at the Indian Institute of Technology – Kharagpur, Kharagpur 721302, INDIA. He is the speaker and corresponding author of this paper. (E-mail: saikat@che.iitkgp.ernet.in).

ISBN: 978-988-19251-5-2
ISSN: 2078-0958 (Print); ISSN: 2078-0966 (Online)

pathway uses flavin as an electron carrier for the reduction of MetHb coupled with NADPH oxidation, catalyzed by NADPH-dependent flavin reductase (FR) ("flavin-NADPH system").

II. Mathematical Modeling

A. Micro Scale

The diffusion-reaction equations in Lagrangian coordinates for a single RBC of any arbitrary shape with volume Ω and external surface area $\partial\Omega$ are given by [7, 8]

$$\alpha_{O_2}\frac{\partial P_{O_2,RBC}}{\partial t} = D_{O_2}\alpha_{O_2}\nabla^2 P_{O_2,RBC} - R_1, \quad (5)$$

$$[Hb]_T\frac{\partial S_{O_2}}{\partial t} = D_{Hb}[Hb]_T\nabla^2 S_{O_2} + R_1 - R_2, \quad (6)$$

$$\alpha_{NO}\frac{\partial P_{NO,RBC}}{\partial t} = D_{NO}\alpha_{NO}\nabla^2 P_{NO,RBC} - (R_2 + R_3), \quad (7)$$

$$[Hb]_T\frac{\partial S_{MetHb}}{\partial t} = D_{Hb}[Hb]_T\nabla^2 S_{MetHb} + R_2, \quad (8)$$

$$[Hb]_T\frac{\partial S_{HbNO}}{\partial t} = D_{Hb}[Hb]_T\nabla^2 S_{HbNO} + R_3, \quad (9)$$

where $P_{i,rbc}$ is the partial pressure of the physically dissolved gas *'i'* (NO or O_2) in the RBC, S_j is the fractional saturation of *'j'* (HbO_2, MetHb, or HbNO) in the hemoglobin, ∇^2 is the three dimensional Laplacian in the local coordinate in the RBC, D_i and D_{Hb} are the diffusion coefficients of gas *'i'* and hemoglobin, respectively, inside the RBC, R_j is the net rate of conversion for corresponding reaction for the compound *'j'*, $[Hb]_T$ is the total intra-erythrocytic hemoglobin (free + bound), and α_i is the solubility of gas *'i'* in the RBC. The uptake rate of oxygen depends on the alveolar partial pressure of oxygen, $P_{A,O2}$, which is typically around 100-110 Torr at STP.

We perform spatial averaging of the above equations over the volume of a single RBC using the Liapunov-Schmidt based spatial-averaging method ([7, 8]). Due to space constraints, we skip the detailed derivation and present the final models we obtained for the micro- and meso-scales. Post spatial-averaging, the micro-scale model for simultaneous reactive uptake of O_2 and NO in RBC is obtained as

$$\left(\alpha_1 + [Hb]_T\beta_{11}\right)\frac{D\overline{P_{1,RBC}}}{Dt} = \Theta_{11}\left(\overline{P_{1,pl}} - \overline{P_{1,RBC}}\right) + \Theta_{12}\left(\overline{P_{2,pl}} - \overline{P_{2,RBC}}\right), \quad (10)$$

$$\left(\alpha_2 + [Hb]_T(\beta_{22} + \beta_{32})\right)\frac{D\overline{P_{2,RBC}}}{Dt} = \Theta_{21}\left(\overline{P_{1,pl}} - \overline{P_{1,RBC}}\right) + \Theta_{22}\left(\overline{P_{2,pl}} - \overline{P_{2,RBC}}\right), \quad (11)$$

where, $\beta_{ij} = \partial S_i / \partial P_{j,rbc}$, α_i is the solubility of gas '*i*' in the RBC, and $\overline{P_{i,RBC}}$ and $\overline{P_{i,pl}}$ are the spatially averaged partial pressures of gas '*i*' in the RBC and the plasma, respectively. The quantity Θ_{ij} is called 'Diffusing Capacity' [7], which represents the reaction-altered mass transport coefficient of gas '*i*' under the driving force of gas '*j*' in the presence of simultaneous reaction and molecular diffusion. The expressions for Θ_{ij} *(i=1,2)* have been derived to be

$$\Theta_{11} = \frac{(\alpha_1 + \beta_{11}[Hb]_T)}{b(\alpha_1 D_1/\eta_1 + b/Sh_i)}G_{11}, \quad (12)$$

$$\Theta_{12} = \frac{(\alpha_1 + \beta_{11}[Hb]_T)}{b(\alpha_2 D_2/\eta_1 + b/Sh_i)}G_{12}, \quad (13)$$

$$\Theta_{21} = \frac{(\alpha_1 + (\beta_{22} + \beta_{32})[Hb]_T)}{b(\alpha_1 D_1/\eta_2 + b/Sh_i)}G_{21}, \quad (14)$$

$$\Theta_{22} = \frac{(\alpha_2 + (\beta_{22} + \beta_{32})[Hb]_T)}{b(\alpha_2 D_2/\eta_2 + b/Sh_i)}G_{22}, \quad (15)$$

where η_i is a mass transfer coefficient of gas '*i*' in the plasma boundary layer surrounding the RBC [7] and G_{ij} is a function of β_{ij} (slope of the saturation curve) .

B. Meso Scale

Our meso-scale analysis is essentially a study of O_2 and NO profiles along a representative pulmonary capillary. The mass transport in the capillary is governed by three modes, namely the averaged partial pressure of gas in the blood plasma, $\overline{P_{i,pl}}$, the cup-mixing partial pressure of the gas, $P_{pl,m,i}$, (which is the velocity weighted average of the partial pressure), and the pressure inside the RBC, $\overline{P_{i,RBC}}$ – the micro-scale variable that affects the meso-scale due to scale coupling. The overall global convection-diffusion-reaction (CDR) equations for gas transport in the plasma are given by

For O_2:

$$\begin{aligned}&(1-h)\left(\frac{\partial C_{pl,O_2}}{\partial t} + v_{pl}(r,x)\frac{\partial C_{pl,O_2}}{\partial x} + R_{pl}C_{pl,O_2}\right)\\ &+h\Theta_{11}\left(\overline{P_{pl,O_2}} - \overline{P_{RBC,O_2}}\right) + h\Theta_{12}\left(\overline{P_{pl,NO}} - \overline{P_{RBC,NO}}\right)\\ &= (1-h)D_{O_2,pl}\left[\frac{1}{r}\frac{\partial}{\partial r}\left(r\frac{\partial C_{pl,O_2}}{\partial r}\right) + \frac{\partial^2 C_{pl,O_2}}{\partial x^2}\right],\end{aligned} \quad (16)$$

For NO:

$$\begin{aligned}&(1-h)\left(\frac{\partial C_{pl,NO}}{\partial t} + v_{pl}(r,x)\frac{\partial C_{pl,NO}}{\partial x} + R_{pl}C_{pl,NO}\right)\\ &+h\Theta_{21}\left(\overline{P_{pl,O_2}} - \overline{P_{RBC,O_2}}\right) + h\Theta_{22}\left(\overline{P_{pl,NO}} - \overline{P_{RBC,NO}}\right)\\ &= (1-h)D_{NO,pl}\left[\frac{1}{r}\frac{\partial}{\partial r}\left(r\frac{\partial C_{pl,NO}}{\partial r}\right) + \frac{\partial^2 C_{pl,NO}}{\partial x^2}\right],\end{aligned} \quad (17)$$

where h is the hematocrit (volume fraction of RBC in blood), $C_{pl,i}$ and $D_{pl,i}$ are the concentration and effective diffusivity, respectively, of the gas i in plasma phase and v_{pl} is the velocity profile of blood in the capillary. The above model is subject to the following boundary conditions:

ISBN: 978-988-19251-5-2
ISSN: 2078-0958 (Print); ISSN: 2078-0966 (Online)

$$-\frac{2}{a}(1-h)D_{i,pl}\frac{\partial C_{pl,i}}{\partial r}=\frac{D_{M,i}}{V_c}(P_{A,i}-P_{pl,i}\big|_{r=a}), \quad (18)$$

$$\frac{\partial C_{pl,i}}{\partial r}=0, \quad (19)$$

where $D_{M,i}$ is the membrane diffusive capacity of gas i, V_c is the capillary bed volume and a is the capillary radius. The meso-scale CDR equations (eqns. 17-19) are subjected to Liapunov-Schmidt spatial averaging over the radius of the pulmonary capillary in order to reduce the dimensionality of the model and the computational effort required to solve it. Subsequently, we employ the assumptions of no reaction occurring in the plasma, and a parabolic laminar velocity profile within the capillary, and non-dimensionalize the spatially-averaged *steady-state* equation system. On doing so, we obtain two global equations given by eqn. (20a) (which are ODEs) and four local equations (two for each gas) given by eqn. (20b) (which are algebraic in nature). Thus, the meso-scale model given by eqn. (20) is a set of Differential Algebraic Equations (DAEs), which must be solved in conjunction with the Eulerian form of the dimensionless micro-scale equations (eqn. 21).

Meso-scale Global Equations:

$$\begin{aligned}(1-h)\frac{dp_{1,m}}{dz}&=\Theta_{1,m}(1-p_{1,s})-h\Theta_{rbc,11}(\overline{p_{1,pl}}-\overline{p_{1,rbc}})\\&\quad-h\Theta_{rbc,12}(\overline{p_{2,pl}}-\overline{p_{2,rbc}}),\\(1-h)\frac{dp_{2,m}}{dz}&=\Theta_{2,m}(k-p_{2,s})-h\Theta_{rbc,21}(\overline{p_{1,pl}}-\overline{p_{1,rbc}})\\&\quad-h\Theta_{rbc,22}(\overline{p_{2,pl}}-\overline{p_{2,rbc}}),\end{aligned} \quad (20a)$$

Meso-scale Local Equations:

$$\begin{aligned}p_{1,m}&=\overline{p_1}-Pe_{T,1}\left[\frac{\Theta_{1,m}}{24}(1-p_{1,s})+\frac{(1-h)}{48}\frac{dp_{1,m}}{dz}\right],\\p_{2,m}&=\overline{p_2}-Pe_{T,2}\left[\frac{\Theta_{2,m}}{24}(k-p_{2,s})+\frac{(1-h)}{48}\frac{dp_{2,m}}{dz}\right],\\p_{1,s}&=\overline{p_1}+\frac{Pe_{T,1}}{24}\left[3\Theta_{1,m}(1-p_{1,s})+(1-h)\frac{dp_{1,m}}{dz}\right],\\p_{2,s}&=\overline{p_2}+\frac{Pe_{T,2}}{24}\left[3\Theta_{2,m}(k-p_{2,s})+(1-h)\frac{dp_{2,m}}{dz}\right],\end{aligned} \quad (20b)$$

Micro-scale Equations:

$$\begin{aligned}\frac{(\alpha_1+[Hb]_T\beta_{11})u_{rbc}}{\tau}\frac{d\overline{p_{rbc,1}}}{dz}&=\Theta_{11}(\overline{p_1}-\overline{p_{rbc,1}})\\&\quad+\Theta_{12}(\overline{p_1}-\overline{p_{rbc,1}}),\\\frac{\{\alpha_2+[Hb]_T(\beta_{22}+\beta_{32})\}u_{rbc}}{\tau}\frac{d\overline{p_{rbc,2}}}{dz}&=\\\Theta_{21}(\overline{p_1}-\overline{p_{rbc,1}})+\Theta_{22}(\overline{p_1}-\overline{p_{rbc,1}}),&\end{aligned} \quad (21)$$

where $p_{i,m}$ is the cup-mixing partial pressure, $p_{i,s}$ is the steady-state pressure at the capillary-membrane interface, $\overline{p_{i,rbc}}$ and $\overline{p_{i,pl}}$ are the spatially averaged dimensionless partial pressures of gas 'i' in the RBC and the plasma, respectively. The quantities Θ_{rbc} and Θ_m are the non-dimensional diffusion capacities of the micro-scale and the capillary membrane, respectively, while Pe_T is the transverse Peclet Number in the pulmonary capillary. Pe_T usually has a value ~10^{-4}, which justifies the use of a low-dimensional description, both qualitatively and quantitatively [8]. The parameter k is the ratio between the alveolar partial pressures of Oxygen and Nitric Oxide, and is of the order of 10^{-6} in this analysis.

C. Solution of Coupled Micro and Meso Scale

The coupled two-scale DAE system results in an ill-conditioned matrix that is hard to handle, even with standard tools such as MATLAB. So, we exploit the linear interdependency of the modes in the meso-scale local equations (eqn. 20b) to convert the system of DAEs into a system of 4 coupled ODEs that describe the coupled two-scale process in terms of partial pressure in the RBC (which is representative of the micro-scale) and cup-mixing partial pressure in the plasma (which is representative of the meso-scale). This set of coupled ODEs is given by

$$\begin{aligned}X_1\frac{dp_{1,m}}{dz}+Y_1\frac{dp_{2,m}}{dz}&=Z_1,\\X_2\frac{dp_{1,m}}{dz}+Y_2\frac{dp_{2,m}}{dz}&=Z_2,\\\overline{X_1}\frac{dp_{1,m}}{dz}+\overline{Y_1}\frac{dp_{2,m}}{dz}+\frac{d\overline{p_{rbc,1}}}{dz}&=\overline{Z_1},\\\overline{X_2}\frac{dp_{1,m}}{dz}+\overline{Y_2}\frac{dp_{2,m}}{dz}+\frac{d\overline{p_{rbc,2}}}{dz}&=\overline{Z_2},\end{aligned} \quad (22)$$

where

$$\begin{aligned}X_1&=1+\frac{3Pe_{T,1}}{8B_1}\Theta_{1,m}+h\Theta_{rbc,11}\left(\frac{Pe_{T,1}}{8B_1}+\frac{\Theta_{1,m}Pe_{T,1}^2}{192B_1}\right),\\Y_1&=h\Theta_{rbc,12}\left(\frac{Pe_{T,2}}{8B_2}+\frac{\Theta_{2,m}Pe_{T,2}^2}{192B_2}\right),\\Z_1&=\frac{\Theta_{1,m}}{(1-h)}\left(1-\frac{6p_{1,m}+\Theta_{1,m}Pe_{T,1}}{B_1}\right)-\\&\frac{h}{1-h}\left[\begin{array}{l}\Theta_{rbc,11}\left(\frac{3p_{1,m}(8+\Theta_{1,m}Pe_{T,1})+\Theta_{1,m}Pe_{T,1}}{4B_1}-\overline{p_{rbc,1}}\right)+\\\Theta_{rbc,12}\left(\frac{3p_{2,m}(8+\Theta_{2,m}Pe_{T,2})+k\Theta_{2,m}Pe_{T,2}}{4D_2}-\overline{p_{rbc,2}}\right)\end{array}\right],\end{aligned} \quad (23)$$

$$\begin{aligned}X_2&=h\Theta_{rbc,21}\left(\frac{Pe_{T,1}}{8B_1}+\frac{\Theta_{1,m}Pe_{T,1}^2}{192B_1}\right),\\Y_2&=1+\frac{3Pe_{T,2}}{8B_2}\Theta_{2,m}+h\Theta_{rbc,22}\left(\frac{Pe_{T,2}}{8B_2}+\frac{\Theta_{2,m}Pe_{T,2}^2}{192B_2}\right),\\Z_2&=\frac{\Theta_{2,m}}{(1-h)}\left(k-\frac{6p_{2,m}+k\Theta_{2,m}Pe_{T,2}}{B_2}\right)\\&-\frac{h}{1-h}\left[\begin{array}{l}\Theta_{rbc,21}\left(\frac{3p_{1,m}(8+\Theta_{1,m}Pe_{T,1})+\Theta_{1,m}Pe_{T,1}}{4B_1}-\overline{p_{rbc,1}}\right)+\\\Theta_{rbc,22}\left(\frac{3p_{2,m}(8+\Theta_{2,m}Pe_{T,2})+k\Theta_{2,m}Pe_{T,2}}{4B_2}-\overline{p_{rbc,2}}\right)\end{array}\right],\end{aligned} \quad (24)$$

where $B_1=(6+Pe_{T,1}\Theta_{1,m})$ and $B_2=(6+Pe_{T,2}\Theta_{2,m})$, and the presence of the small parameter k (=10^{-6}) (as well as in the

ISBN: 978-988-19251-5-2
ISSN: 2078-0958 (Print); ISSN: 2078-0966 (Online)

equations below) introduces a large difference of magnitude between the micro- and meso scales.

The solution of the system of ODEs (eqn. 22-26) was performed using MATLAB. The mass matrix being extremely stiff and ill-conditioned due to the large difference in variable values at the two scales, appropriate stiff solvers were employed.

$$\begin{aligned}
\overline{X_1} &= -\frac{(1-h)\tau}{u_{rbc}(\alpha_1+[Hb]_T\beta_{11})}\Theta_{11}\left(\frac{Pe_{T,1}}{8B_1}+\frac{\Theta_{1,m}Pe_{T,1}^{\ 2}}{192B_1}\right),\\
\overline{Y_1} &= -\frac{(1-h)\tau}{u_{rbc}(\alpha_1+[Hb]_T\beta_{11})}\Theta_{12}\left(\frac{Pe_{T,2}}{8B_2}+\frac{\Theta_{2,m}Pe_{T,2}^{\ 2}}{192B_2}\right),\\
\overline{Z_1} &= \frac{(1-h)\tau}{u_{rbc}(\alpha_1+[Hb]_T\beta_{11})}\\
&\left[\begin{array}{l}\Theta_{11}\left(\dfrac{3p_{1,m}(8+\Theta_{1,m}Pe_{T,1})+\Theta_{1,m}Pe_{T,1}}{4B_1}-\overline{p_{rbc,1}}\right)+\\ \Theta_{12}\left(\dfrac{3p_{2,m}(8+\Theta_{2,m}Pe_{T,2})+k\Theta_{2,m}Pe_{T,2}}{4B_2}-\overline{p_{rbc,2}}\right)\end{array}\right],
\end{aligned} \tag{25}$$

$$\begin{aligned}
\overline{X_2} &= -\frac{(1-h)\tau}{u_{rbc}\{\alpha_1+[Hb]_T(\beta_{22}+\beta_{32})\}}\Theta_{21}\left(\frac{Pe_{T,1}}{8B_1}+\frac{\Theta_{1,m}Pe_{T,1}^2}{192B_1}\right),\\
\overline{Y_2} &= -\frac{(1-h)\tau}{u_{rbc}\{\alpha_1+[Hb]_T(\beta_{22}+\beta_{32})\}}\Theta_{22}\left(\frac{Pe_{T,2}}{8B_2}+\frac{\Theta_{2,m}Pe_{T,2}^2}{192B_2}\right),\\
\overline{Z_2} &= \frac{(1-h)\tau}{u_{rbc}\{\alpha_1+[Hb]_T(\beta_{22}+\beta_{32})\}}\\
&\left[\begin{array}{l}\Theta_{21}\left(\dfrac{3p_{1,m}(8+\Theta_{1,m}Pe_{T,1})+\Theta_{1,m}Pe_{T,1}}{4B_1}-\overline{p_{rbc,1}}\right)+\\ \Theta_{22}\left(\dfrac{3p_{2,m}(8+\Theta_{2,m}Pe_{T,2})+k\Theta_{2,m}Pe_{T,2}}{4B_2}-\overline{p_{rbc,2}}\right)\end{array}\right].
\end{aligned} \tag{26}$$

We may note that the differences at the capillary and RBC levels are related more to the disparity in characteristic time scales rather than that of the length scales. All the three reactions are extremely fast (as indicated by the reaction rate constants provided below). Next to reaction, radial diffusion has the shortest time scales (approximately 0.006 s), followed by the capillary transit time of blood (τ =1 s) .The axial diffusion time scale (approximately 1000 s) is significantly larger than the rest of the time scales. The values of the various constants used in the analysis are K_1=2.648×10^{10} s^{-1}, K_2=2.1×10^9 s^{-1}, K_3=3.4×10^9 s^{-1}, n=2.37, $\alpha_{O2,RBC}$ =1.56×10^{-6} mol/Torr, $\alpha_{NO,RBC}$ =2.58×10^{-6} mol/Torr, $D_{O2,RBC}$ =9.5×10^{-6} cm^2/s, $D_{NO,RBC}$ =3.5×10^{-5} cm^2/s, D_{Hb} =1.44x10^{-7} cm^2/s, $D_{O2,pl}$ =2.5×10^{-5} cm^2/s, $D_{NO,pl}$ =2.5×10^{-5} cm^2/s, V_c=60 c.c., $D_{M,O2}$=40 Torr^{-1}min^{-1}, $D_{M,NO}$=22 Torr^{-1}min^{-1}, where D_{pl} and D_m refer to effective diffusivity of the gas in the plasma and diffusive capacity for transport through the capillary membrane, respectively. $D_{O2,m}$ is based on literature [7]. The value of $D_{M,NO}$ is calculated by using $\frac{D_{M,NO}}{D_{M,O_2}} \approx \frac{\text{Membrane diffusivity of NO}}{\text{Membrane diffusivity of O}_2}$.

The value for the diffusivity of oxygen in membranes has been found to be $0.727\text{x}10^{-5}\,\text{cm}^2/\text{s}$ [13] and that for NO has been estimated at $0.4\text{x}10^{-5}\,\text{cm}^2/\text{s}$ [14].

III. Results and Discussion

We use deoxygenated blood with an oxygen partial pressure of 40 Torr in the RBC, 42 Torr in the plasma and S_{HbO2}=75% as initial conditions for our simulation. Figure 1(a) presents the simulated profile for oxygen saturation in the rbc (S_{HbO2}) along the capillary for different values of alveolar partial pressure of Nitric Oxide. The figure shows that when the value of alveolar NO is nearly zero, oxygen saturation attains equilibrium at 97% and the oxygen tension increases to 110 Torr. Oxygen diffuses through the membrane separating the air and the blood from the high partial pressure in the alveoli (110 Torr) to the area of lower partial pressure in the pulmonary capillaries (40-42 Torr). For this case, the oxygen saturation reaches a steady state within 15-20 % of the total capillary length of 0.1 cm. It may be mentioned that S_{HbO2}=90% in the arterial (oxygenated) blood is considered to be the critical oxygen saturation required for the patient to survive. Thus, we note from Fig. 1 that in the presence of alveolar NO in methemoglobinemia patients, this critical oxygen saturation (~90%) occurs when the alveolar NO concentration is 150ppm or above.

Figure 1(b) shows the profile for the total NO saturation in the RBC, S_{NO} ($=S_{MetHb}$ + S_{HbNO}) along the length of the pulmonary capillary. The steady state is attained at 20% of the total capillary length.

Figures 2(a) and 2(b) show the individual saturations (along the capillary) of the two components of reacted NO in the hemoglobin, namely Nitrosylhemoglobin (*HbNO*) and Methemoglobin (*MetHb*), respectively. As discussed before, the level of *MetHb* in normal hemoglobin is known to be 1%. However, it may observed from Fig. 2(b) that as the concentration of NO in the RBC increases, *MetHb* saturation increases significantly to about 6% (in the critical case), leading to the onset of methemoglobinemia.

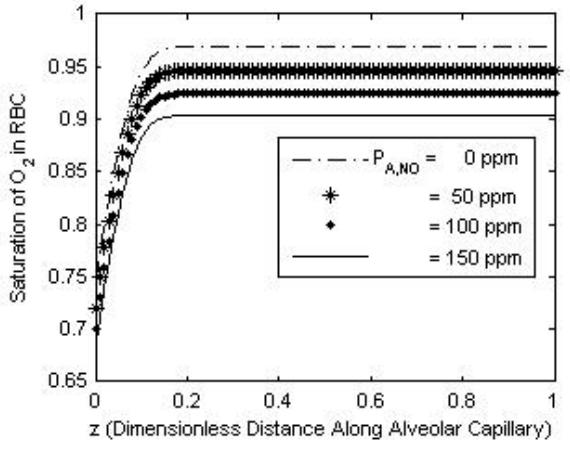

ISBN: 978-988-19251-5-2
ISSN: 2078-0958 (Print); ISSN: 2078-0966 (Online)

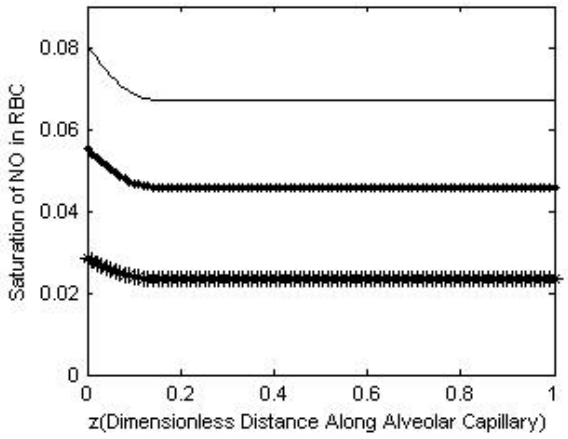

Fig.1. Profiles of (a) S_{HbO2} and (b) S_{NO} inside RBC (along the capillary length) for different values of alveolar NO concentration ($P_{A,NO}$).

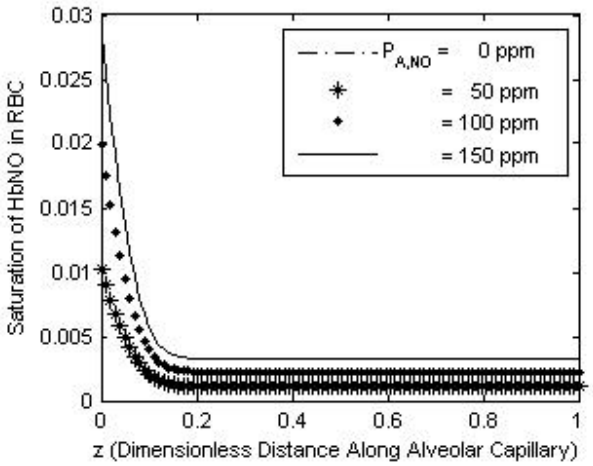

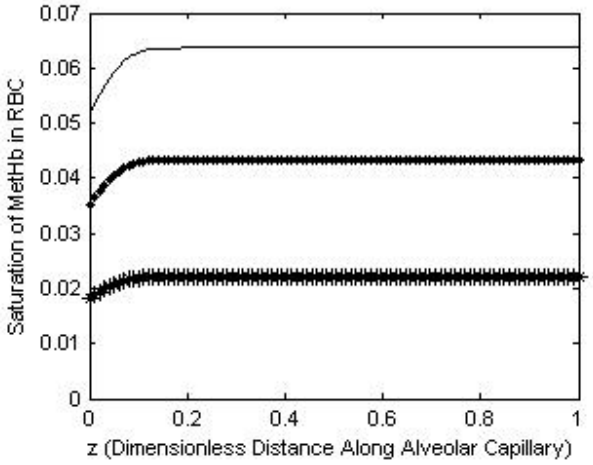

Fig.2. Profiles of (a) S_{HbNO} and (b) S_{MetHb} inside RBC along the capillary length for different values of alveolar NO concentration ($P_{A,NO}$).

Figures 3(a) and 3(b) present the variation of the partial pressures of Oxygen in the RBC and the plasma, respectively, along the capillary length for different values of alveolar NO concentration. We note that for both the micro- and meso-scales, steady states are attained at around 20% of the capillary distance for an alveolar pressure of 110 mmHg. Thus, the oxygen partial pressure in the RBC and plasma are not significantly affected by changes in alveolar concentration of NO but oxygen saturation is strongly dependent on it, as is evident from Fig. 1(a). It may also be noted that the partial pressure of Oxygen inside the RBC always remains slightly lower than that inside the plasma so that a diffusional gradient exists until equilibrium is attained. Though intuitively obvious, we shall soon see that this does not hold true for Nitric Oxide.

Figures 4(a) and 4(b) show the profiles of the partial pressures of Nitric Oxide at the meso (capillary) and micro (RBC) scale. A close look at the magnitudes at which equilibration occurs shows that the pressure inside the RBC, though initially lower steadies at a slightly higher value than that in the plasma. This could be attributed to the interesting dynamics of convection, diffusion and reaction that the two scales with widely differing time-scales are locked into.

The system of equations that were obtained and solved takes into account the three reactions (1), (2) and (3) that describe the kinetic interaction of Nitric Oxide and Oxygen

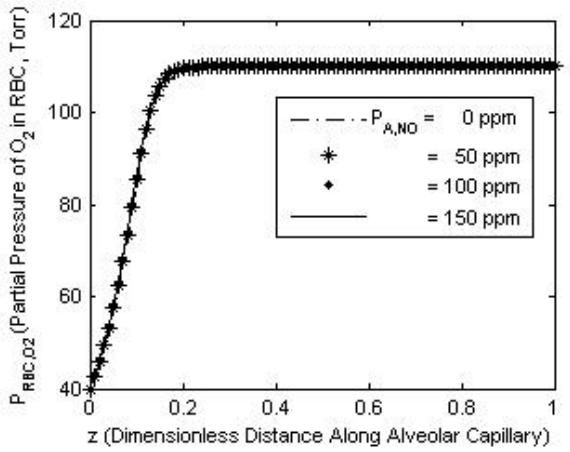

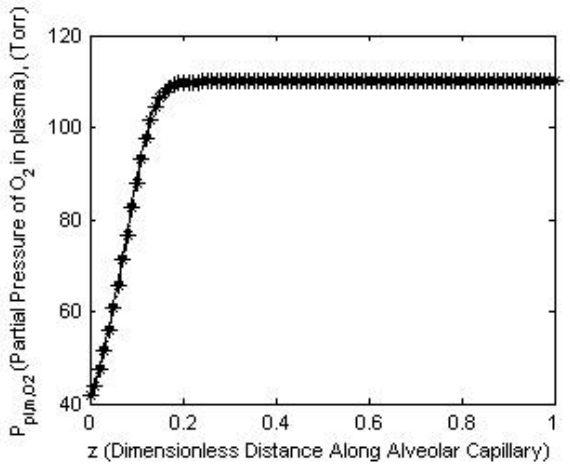

Fig.3. Profiles of (a) $P_{RBC,\,O_2}$ (inside RBC) and (b) P_{pl,m,O_2} along the capillary for different values of alveolar NO concentration ($P_{A,NO}$).

with Hemoglobin in the RBC. For NO concentration above 150 ppm, the patient needs to be treated with methylene blue, which works as a cofactor for the enzyme NADPH-methemoglobin reductase that helps in rapid conversion of MetHb back to Hb. In that case, the kinetic model would include one more reaction (in addition to eqns. 1-3) given by

$MetHb + MetHb - reductase(red.) \Leftrightarrow Hb + MetHb(ox.)$, and

the CDR model (eqn. 5-9) and the subsequent spatially-averaged low-dimensional analyses would have to be

ISBN: 978-988-19251-5-2
ISSN: 2078-0958 (Print); ISSN: 2078-0966 (Online)

modified accordingly. The dynamics of the therapy of methemoglobinemia using a similar multiscale approach shall be examined in our future publications.

IV. Conclusions

In order to quantify hypoxemia in methemoglobinemia, we start with the fundamental convection-diffusion-reaction equations and derive a coupled two (micro-meso) scale model for coupled reactive transport of nitric oxide and oxygen in the red blood cell and the pulmonary capillary. The rate equations for reactions of NO with oxy- and deoxy-hemoglobin are developed and incorporated in the diffusion-reaction model. The three-dimensional model equations both at the micro and at the meso scales are spatially averaged using the Liapunov-Schmidt technique of the classical bifurcation theory to obtain low-dimensional models that include analytical expressions for O_2 and NO diffusing capacities in the RBC for the case of continuous exposure to these gases.

The numerical solution of our coupled two-scale model shows that for NO concentration above 150 ppm, oxygen saturation falls below the critical limit of 90% required for the human body to function. Thus, we find that an alveolar NO concentration of 150ppm or higher in methemoglobinemia patients would be fatal, if not provided with immediate therapy. We also find that while oxygen partial pressures in both the RBC and plasma are seen to be extremely weak functions of the alveolar NO levels, the oxygen saturation is significantly and often fatally affected. Thus, our model simulations reveal that the diagnosis of hypoxemia in methemoglobinemia cannot be done by measuring oxygen partial pressures in the patient's pulmonary artery but by measuring the oxygen saturation in the patient's erythrocyte using pulse oximetry. Further, we briefly discuss the commonly-used therapeutic approach for methemoglobinemia and outline the changes that need to be incorporated in our kinetic and transport models to quantify the dynamics of the therapeutic process using this multiscale analysis.

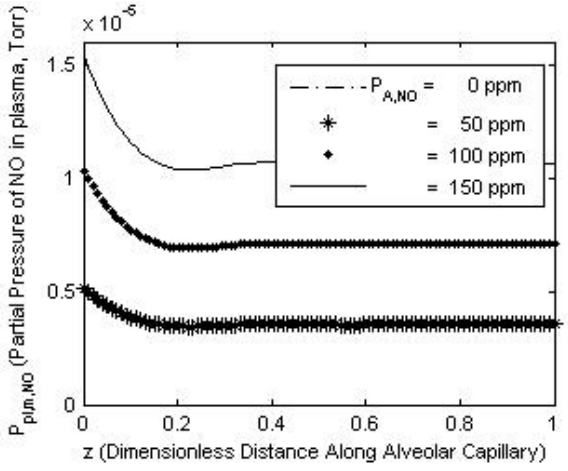

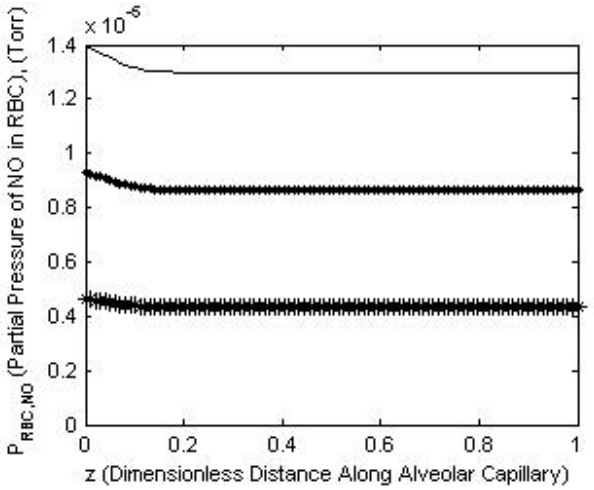

Fig.4. Profiles of (a) $P_{RBC,\,NO}$(inside RBC) and (b) $P_{pl,m,NO}$ along the capillary for different values of alveolar NO concentration ($P_{A,NO}$).

References

[1] Eich R.F., Li T., Lemon D.D., Doherty D.H., Curry S.R., Aitken J.F., Mathews A.J., Johnson KA, Smith RD, Phillips GN Jr, Olson JS., 1996. Mechanism of NO-induced oxidation of myoglobin and hemoglobin. Biochemistry. 35(22):6976-83.

[2] Scheele J.S., Burner E., Kharitonov V.G., Martasek P., Roman L.J., Masters B.S.S., Simulation Study for Methemoglobin Reduction Pathways.http://www.ncbi.nlm.nih.gov/books/bv.fcgi?indexed=google&rid=eurekah.section.74876

[3] Power G.G., Bragg S.L., Oshiro B.T., Dejam A., Hunter C.J., and Blood A.B., 2007. A novel method of measuring reduction of nitrite-induced methemoglobin applied to fetal and adult blood of humans and sheep. Journal of Applied Physiology. 103(4):1359-65

[4] Azizia F., Kielbasaa J.E., Adeyigaa A.M., Mareea R.D., Fraziera M., Yakubuk M., Shieldsa H., Kingd S.B.and Kim-Shapiro A.E., 2005. Rates of nitric oxide dissociation from hemoglobin. Free Radical Biology & Medicine 39 145-151.

[5] Kuma F.,1981. Properties of methemoglobin reductase and kinetic study of methemoglobin reduction, J Biol Chem.256:5518-23.

[6] Abe K. and Sugita Y., 1979. Properties of cytochrome b5 and methemoglobin reduction in human erythrocytes, Eur J Biochem.101:423-8.

[7] Chakraborty S., Balakotaiah V., and Bidani A., 2004. Diffusing capacity reexamined: relative roles of diffusion and chemical reaction in red cell uptake of O2, CO, CO2 and NO. Journal of Applied Physiology, 97: 2284-2302.

[8] Chakraborty S., Balakotaiah V., and Bidani A., 2007. Multiscale model for pulmonary oxygen uptake and its application to quantify hypoxemia in hepatopulmonary syndrome. Journal of Theoretical Biology 244 ,190–207.

[9] Higasa K, Manabe JI, Yubisui T, Sumimoto H, Pung-Amritt P, Tanphaichitr VS, Fukumaki Y., 1998. Molecular basis of hereditary methaemoglobinaemia, types I and II: two novel mutations in the NADH-cytochrome b5 reductase gene. Br. J Haematol. 103: 922-30.

[10] Boylston M. and Beer D., 2002. Methemoglobinemia: A Case Study. Crit Care Nurse; 22(4): 50-55.

[11] Lurie M.A., 1993. A Concise review: Methemoglobinemia. Am J Hematol; 42:7.

[12] Turner M.D., Karlis V., and Glickman R.S., 2007, The Recognition, Physiology, and Treatment of Medication-Induced Methemoglobinemia: A Case Report. Anesth Prog. 2007 Fall; 54(3): 115–117.

[13] Lissi E.A. and Caceres T., 1989, Oxygen Diffusion-Concentration in Erythrocyte Plasma Membranes Studied by the Fluorescence Quenching of Anionic and Cationic Pyrene Derivatives. Journal of Bioenergetics and Biomembranes; 21(3): 375-385

[14] Denicola A, Souza JM, Radi R, Lissi E., 1996, Nitric oxide diffusion in membranes determined by fluorescence in quenching. Arch Biochem Biophys; 328(1):208-212

ISBN: 978-988-19251-5-2
ISSN: 2078-0958 (Print); ISSN: 2078-0966 (Online)